Microchemical Journal 214 (2025) 113934

Contents lists available at ScienceDirect

Microchemical Journal

journal homepage: www.elsevier.com/locate/microc

Estimation of the critical micelle concentration of sodium taurocholate in intestine-relevant conditions using complimentary techniques

Susana Amézqueta [a,*], Unai Casanova [a], Elisabet Fuguet [a,b], Clara Ràfols [a]

[a] Departament d'Enginyeria Química i Química Analítica and Institut de Biomedicina (IBUB), Facultat de Química, Universitat de Barcelona, Martí i Franquès 1-11, 08028 Barcelona, Spain
[b] Serra Húnter Programme, Generalitat de Catalunya, Spain

ARTICLE INFO

Keywords:
Intestinal biorelevant media
Micellization
Conductimetry
Fluorescence
Isothermal titration calorimetry
Sodium taurocholate
Critical micelle concentration

ABSTRACT

Bile salts such as sodium taurocholate (NaTc) play an important role in drugs' bioavailability due to their capacity to form micelles. These aggregates can host a wide range of drugs and enhance their solubility in biological fluids. The micellization process and the types of micelles formed not only depend on the surfactant, but also on the environment (solvent, temperature, presence of other compounds, etc.). Therefore, when solubility assays are performed it is key to ensure that micelles are present. In this work, the critical micelle concentration (CMC) of NaTc has been evaluated using three different techniques (conductometry, fluorescence and calorimetry) in water and in different biorelevant conditions (intestinal biorelevant aqueous buffers, FaSSIF-v2 and FeSSIF-v2). While conductometry is not adequate for CMC determination of bile salts, fluorescence and calorimetry offer complementary information. CMC experiments have shown that ion strength and the presence of mixed micelles (formed by NaTc, phosphatidylcholine and lipids) favor the micellization process and would impact on the drugs bioavailability.

1. Introduction

Bile salts are compounds formed primarily in the liver by the oxidation of cholesterol and stored in the gallbladder. In concrete, sodium taurocholate (NaTc) (Fig. 1) results from the conjugation of a primary bile acid (cholic or chenodeoxycholic acid) and taurine. These compounds play an important role in the digestion and the absorption of lipophilic compounds due to their function as biosurfactants [1]. Also, they are appreciated due to their ability to modify enzyme catalytic activity when combined with phospholipids in form of mixed micelles [2], to act as chiral selectors in chromatography applications [3] and to act as solubilization and dispersive agents in the preparation of nanotechnology functional materials [4].

Conventional surfactants such as sodium dodecyl sulfate (SDS) self-aggregate when a specific concentration, called critical micelle concentration (CMC), is reached. Bile salts also form micelles, although they aggregate more gradually, and have a smaller aggregation number, higher charge density and higher polydispersity [5]. Bile salts have a rigid backbone with a curved geometry. The convex side, with methyl groups, is hydrophobic while the concave side, with hydroxyl groups, and the lateral chain are hydrophilic. The molecular rigidity and the far distance between the hydrogen bond sites of the skeleton and the main polar group situated in the lateral chain permits bile salts aggregate. This aggregation is peculiar as the polar and nonpolar regions are not completely separated, and the interactions involved probably might be the result from electrostatic, van der Waals, hydrophobic and steric forces [6,7]. In fact, the exact process remains still unclear, and several models of aggregation have been proposed [5,7]. In the case of NaTc, micelles of around 10 units would coexist with monomers and dimers and could interact transitively with other molecules in a dynamic manner [8].

This process can be studied through different analytical techniques from the monitoring of various physical properties, including heat exchange (calorimetry), surface tension (osmometry), conductivity (conductometry), probe's fluorescence intensity (fluorescence), chemical shift (NMR) and ultrasonic velocity (ultrasounds). In general, the analytical methods compare the differences of the physical property in the premicellar region (solution containing surfactant monomers) and the postmicellar region (solution containing surfactant monomers, small aggregates and micelles in equilibrium). To obtain the CMC value, the

* Corresponding author at: Departament d'Enginyeria Química i Química Analítica, Facultat de Química, Universitat de Barcelona, Martí i Franquès 1-11, 08028 Barcelona, Spain.
E-mail address: samezqueta@ub.edu (S. Amézqueta).

https://doi.org/10.1016/j.microc.2025.113934
Received 3 April 2025; Received in revised form 7 May 2025; Accepted 9 May 2025
Available online 13 May 2025

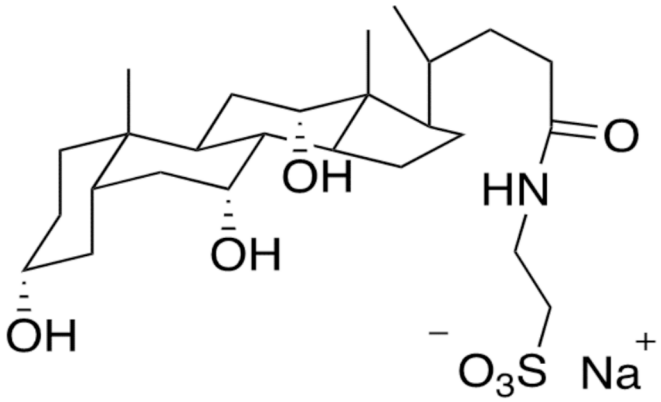

Fig. 1. Sodium taurocholate.

behavior of a physical property in the premicellar and the postmicellar region is compared. Data treatment approaches include the evaluation of the intersection between two straight lines or the inflexion point of a curve, among others [9–11].

Table 1 shows the CMC values of NaTc in water reported in the literature at different temperatures (10–40 °C) and using different analytical methods. In this medium, the CMC value varies in the range 6.1–15 mM. It is important to note that the micellization process is influenced by several factors such as the type of surfactant, the temperature, or the composition, pH and ionic strength of the medium [12]. Therefore, Table 1 also includes the CMC values obtained using different electrolyte systems. They mainly have been evaluated by isothermal titration calorimetry (ITC), and the CMC (in the range 3–13 mM) is more variable than when working with water as more variables are introduced into the system (components, pH, temperature).

Nowadays, drug classification systems stand out the necessity to consider biorelevant conditions in the drugs' formulation strategy. Specifically, the Developability Classification System (DCS) for orally administered drugs, suggests the classification of drugs into five categories depending on their solubility and the estimated effective jejunal permeability in simulated intestinal media [13]. Therefore, the study of micellization using media and components that mimic gastrointestinal tract is key in understanding the solubility and bioavailability of orally administered drugs, specially of those presenting limited solubility in water [14]. Recent studies have also revealed the interest in using intestinal simulated fluids to improve the evaluation of the reabsorption of drugs that can be entrapped in bile micelles during the enterohepatic circulation [15].

Literature reports studies performed considering the pH and ion strength of gastric fluids (pH ~ 3, I ~ 100 mM) or blood (~7.4, I ~ 150 mM), but they do not mimic the fluids were NaTc is mainly present: intestinal fluids (pH 5.8–6.5) (Table 1). Further, it has to be noted that, under physiological conditions, bile salts can also form mixed micelles in the presence of phospholipids and/or other substances (e.g. fatty acids or cholesterol) [7,16]. Thus, the present study will focus on the evaluation of, on one hand, the influence of intestinal fluid conditions (pH and ionic strength) in the CMC of NaTc and, on the other hand, the effect of

Table 1
NaTc CMC values in water or aqueous buffers at different temperatures.

Medium		T (°C)	CMC (mM)	Analytical technique	Ref.
Water		10	6.79	Osmometry	[24]
		20	6.68	Osmometry	[24]
			8–12	Fluorescence	[26]
		25	8.3 (pentamer)	NMR	[37]
			8–12	Fluorescence	[27]
			10.5	Fluorescence	[30]
			13.3	Calorimetry	[30]
		30	6.14	Osmometry	[24]
			10	Ultrasounds	[38]
		32	13.3	Calorimetry	[30]
		35	15	Fluorescence	[28]
		37	15	NMR	[35]
			13.2	Calorimetry	[30]
		40	6.36	Osmometry	[24]
Water +	10 mM NaCl	25	12	Ion electrode	[39]
	15 mM NaCl	35	13	Fluorescence	[28]
	75 mM NaCl		11		[28]
	150 mM NaCl		9		[28]
	300 mM NaCl		8		[28]
Citrate buffer	(100 mM, pH 3.0)	25	6.5	ITC	[40]
			3–4	Osmometry (surface tension)	[40]
Acetate buffer	(100 mM, pH 3.0)	30	12.6 ± 0.9	ITC	[37]
	(100 mM, pH 3.0) + 10 mM NaCl		11.4 ± 0.9	ITC	[37]
	(100 mM, pH 3.0) + 50 mM NaCl		8.8 ± 0.9	ITC	[37]
	(100 mM, pH 3.0) + 150 mM NaCl		7.4 ± 0.9	ITC	[37]
Acetate buffer	(pH 5, I = 389 mM)	37	~3	NMR	[35]
HEPES buffer	(10 mM, pH 7.4) + 145 mM NaCl	n.a.	6.5 ± 0.5	Osmometry (surface tension)	[41]
Phosphate buffer	(pH 7.4) + 150 mM NaCl	25	Near 0	ITC	[42]
	(pH 7.4) + 150 mM NaCl	15, 28, 31, 34, 37	~ 8	ITC	[42]
	(pH 7.4) + 150 mM NaCl	37	8.5	Light scattering	[43]
	(pH 6.5) + 190 mM NaCl	37	~3	NMR	[35]

na: not available

the formation of mixed micelles with other intestinal fluid components on NaTc micellization. Tables A.1 and A.2 (Supplementary material) show the components of intestinal fluids and those of the commercially available simulated intestinal fluids (SIF) that mimic the fasted and the fed states (FaSSIF-v2 and FeSSIF-v2, respectively) [17] and that will be used in the present study.

2. Material and methods

2.1. Equipment

Conductivity measurements were carried out using the CDM 83 conductometer (Radiometer Copenhagen, Denmark) and the CDC114 conductometry cell (Radiometer). Fluorescence was monitored using a Cary Eclipse Fluorescence spectrophotometer from Varian-Agilent Technologies (Santa Clara, CA, USA). To perform the calorimetric measurements, a VP-ITC system controlled by VPViewer2000 from MicroCal (Northampton, Ma, USA) was used.

2.2. Reagents

NaTc, SDS, propranolol hydrochloride, tetracaine, sodium hydroxide, sodium chloride and potassium chloride were from Merck (Darmstadt, Germany); maleic acid was from Carlo Erba (Milan, Italy); FaSSIF-v2 and FeSSIF-v2 were from Biorelevant (London, UK). FaSSIF-v2 powder contains NaTc and lecithin, while FeSSIF-v2 powder contains NaTc, lecithin, glycerol monooleate and sodium oleate [17]. To prepare the solutions, double distilled water obtained from a Milli-Q system from Millipore (Burlington, MA, USA) was used.

2.3. Methods

Each experiment was done at least with three replicates. CMC of NaTC was determined in five different media: water, maleic buffer at pH 6.5, maleic buffer at pH 5.8, FaSSIF-v2, and FeSSIF-v2. Maleic buffer pH and ionic strength are the ones needed to prepare the simulated intestinal fluids (pH 6.5 ($I = 140$ mM), to mimic fasted state, and pH 5.8 ($I = 320$ mM), to mimic fed state), so they were prepared according to Biorelevant instructions [17]. FaSSIF-v2 and FeSSIF-v2 powders were dissolved in maleic buffer pH 6.5 ($I = 140$ mM), and maleic buffer pH 5.8 ($I = 320$ mM), respectively.

The concentration of NaTc (pure or as a component of FaSSIF-v2 and FeSSIF-v2 powders) selected for the stock solution in each analytical method assured the coverage of the premicellar and the postmicellar regions.

2.3.1. Conductometry

First, the conductometer was calibrated using KCl as a standard. A solution of the surfactant (50 mM) was prepared in water or in maleic buffers and placed in a burette. Next, 25 additions of 1 mL of the surfactant solution were performed over the conductometric cell containing 15 mL of water or buffer, and the conductivity was measured after each addition. Experiments were carried out at 25 °C and under vigorous stirring.

2.3.2. Fluorescence

First, probe working solutions (0.06 mM for propranolol and 0.03 mM for tetracaine) and NaTc solutions (300 mM for water and aqueous buffers, and 200 mM for FaSSIF-2 and FeSSIF-v2) were prepared in the desired medium. In each experiment, surfactant and probes were solved in the same medium. To perform the experiments, 3 mL of the probe's solution were placed in the cuvette. Next, 16 consecutive additions of NaTc of 10–15 μL were done in 3 min intervals (time needed to achieve the reaction equilibrium). Fluorescence was recorded using a 1 cm path length quartz QS cuvette (Hellma Analytics, Jena, Germany), 600 nm/min scan speed, and slit widths of 10 nm for both excitation and emission monochromators. Excitation was fixed at 310 nm and emission at 364 nm for NaTc, 349 nm for propranolol and 372 nm for tetracaine. All experiments were carried out at 25 °C.

2.3.3. Isothermal titration calorimetry

A solution of the surfactant (250 mM) was prepared in water or aqueous buffer and placed in the ITC syringe. Accordingly, water or aqueous buffer was placed in the cell (1.4 mL). Both had been previously degassed for 5 min. Next, 30 additions of the stock solution were performed over the cell, and the heat involved in each injection was measured and integrated to be able to calculate the ΔH for each injection. Experiments were carried out at three different temperatures (25, 32 and 37 °C). Before each experiment, the corresponding blank was performed to correct for background heat in the data treatment.

2.4. Calculation methods

2.4.1. Conductometry and fluorescence

The signal (conductivity (κ) or fluorescence (F)) of the sample solution changes as the surfactant concentration increases. In the premicellar region, the surfactant, added through the additions of stock solution, experiments a dilution, and its charged monomers provide the proportional variation of the signal. When the surfactant concentration in the sample solution reaches the CMC, molecules start self-aggregating, and then the signal also changes, proportionally to the surfactant added, but with a different slope. The CMC, point where the slope change occurs, can be calculated using different strategies [10]. In this work, the Carpena's method has been selected as it is the recommended when there is not a sharp transition between the premicellar and the postmicellar regions [10]. This method consists of fitting the sigmoidal Boltzmann equation (Eq. (1) to the experimental data [9] using the least squares method to obtain by iteration [18] parameters related to the micellization process (CMC and ΔC_D).

$$S(C_j) = S_{C=0} + a_1 \times C_j + (a_2 - a_1) \times \Delta C_D \times ln\left(\frac{1 + e^{(C_j - CMC)/\Delta C_D}}{1 + e^{-CMC/\Delta C_D}}\right) \quad (1)$$

In this equation, $S(C_j)$ is either the conductivity or the fluorescence intensity, and C_j is the concentration of surfactant at injection j; $S_{C=0}$ is the value of specific signal (κ or F) when C_j is 0; a_1 and a_2 are the slope of the premicellar and postmicellar linear regions; CMC is the breakpoint of curve S/C_j; and ΔC_D is the width of transition between the premicellar and the postmicellar regions. In the case of FaSSIF-v2 and FeSSIF-v2, where mixed micelles are formed, the concentration of surfactant is expressed as NaTc concentration.

2.4.2. Calorimetry

The method applied in ITC determinations is the one proposed by Tso *et al.* [11], which is an extension of a previous method based on demicellization titrations [19,20]. It evaluates the demicellization process that occurs when a solution of the surfactant (surfactant concentration ≫ CMC) is added to the calorimetric cell containing the solvent. At the beginning of the titration (premicellar region), the break of the micelle and the dilution of the monomers occurs and the corresponding heat is recorded. At the end, when the cell concentration exceeds the CMC (postmicellar region), monomers and micelles coexist in equilibrium and the heat recorded is the one related with the dilution of the newly added micelles. Between these two regions there is a transition region were both processes coexist and the corresponding global heat is measured.

Therefore, most of the ITC demicellization experiments result in a isotherm curve that can be modelled using Eq. (2) [11].

$$Q(C_j) = \frac{\left[(a_1 - a_2)(C_j - CMC)\right] - \left[\Delta H_{mic}(C_{syr} - CMC)/C_{syr}\right]}{1 + e^{(C_j - CMC)/\Delta C_D}} + \\ + \left[a_2(C_j - C_{ref})\right] + b_2 \quad (2)$$

where $Q(C_j)$ and C_j are the heat and concentration of surfactant at injection j; a_1 and a_2 are the slope of the premicellar and postmicellar linear regions, respectively; b_2 is the y-intercept of the postmicellar linear region; ΔH_{mic} is the enthalpy of micellization; CMC is the breakpoint of curve Q/C_j; C_{ref} is the reference concentration of surfactant defined to minimize the correlation of parameters; and C_{syr} is the concentration of surfactant in the syringe; ΔC_D is the width of the transition between the premicellar and the postmicellar regions. Again, in the case of FaSSIF-v2 and FeSSIF-v2 the concentration of surfactant is expressed as NaTc concentration.

The CMC, ΔH_{mic} and a ΔC_D are obtained by fitting Eq. (2) to the experimental isotherm ($Q(C_j)$) by nonlinear least-squares fitting. The approach is implemented using stand-alone software called D/STAIN, which is freely available [21,22].

3. Results and discussion

It is well known that bile salts aggregate gradually, fact that may imply some difficulties in the CMC determination. To be able to compare the micellization of the bile salt NaTc with micellization of conventional surfactants, we first evaluated the CMC of SDS in water by the three different methodologies (conductimetry, fluorescence emission and calorimetry) using the same experimental conditions as for NaTc. The results obtained for SDS agree with those reported in the literature using the same analytical technique (Fig. A.1 and Table A.3 – Supplementary material).

3.1. Conductometry

When working with conventional surfactants such as SDS, a change in the slope is clearly observed at the point where the micelles form (Fig. A.1.a – Supplementary material). In the case of NaTc in water, as shown in Fig. 2, only one type of relationship between the conductivity and the concentration of surfactant added to the cell is observed in the whole work range. This is, the slope is the same in the premicellar and the postmicellar regions and, hence, the micelles formation is not detected.

This phenomenon was also observed by our group of research in previous studies on another bile salt, sodium cholate [23]. Other authors observed a very slight difference in the slopes of the two regions when working with sodium taurocholate [24], sodium deoxycholate and sodium chenodeoxycholate [25]. According to Mukherjee *et al.* [24], the CMC value for NaTc would be around 7–8 mM at 10–40 °C. Natalini *et al.* [25] indicated that bile salt micelles have low aggregation number, and that the binding and inclusion of counterions within the micelles is assumed to be negligible for bile salts. These characteristics may imply that the small bile salts aggregates have a mobility very similar to that of the corresponding monomers [25], making the detection of the breakpoint very difficult.

Furthermore, when we tried to perform the micellization experiments in buffer the current was so high due to the presence of salts that we could not detect the small changes caused by the micelles' formation.

Hence, we consider that this method is not suitable for the determination of the CMC of NaTc and probably of other biliary salts, and that more sensitive techniques should be used.

3.2. Fluorescence

Most of the fluorometric methods reported in the literature for CMC determination use probes [26–28]. Although pyrene is one of the most widely used probes for conventional surfactants [29], it presents some disadvantages for NaTc micellization studies due to the presence of a fluorescence quenching effect during the first additions of surfactant to the system [30]. In a previous work we showed that the CMC of NaTc can be evaluated screening the surfactant itself, but that probes such as propranolol or tetracaine provide more pronounced fluorescence differences between the premicellar and the postmicellar regions, and hence more accurate determinations [30].

Fig. 3 shows I *vs* C_{NaTc} plots in different aqueous media at 25 °C using propranolol as fluorophore (Fig. 3a) or tetracaine (Fig. 3b). In these aqueous solutions, the fluorescence intensity of the fluorophores remains constant or increases slightly upon the first additions of the

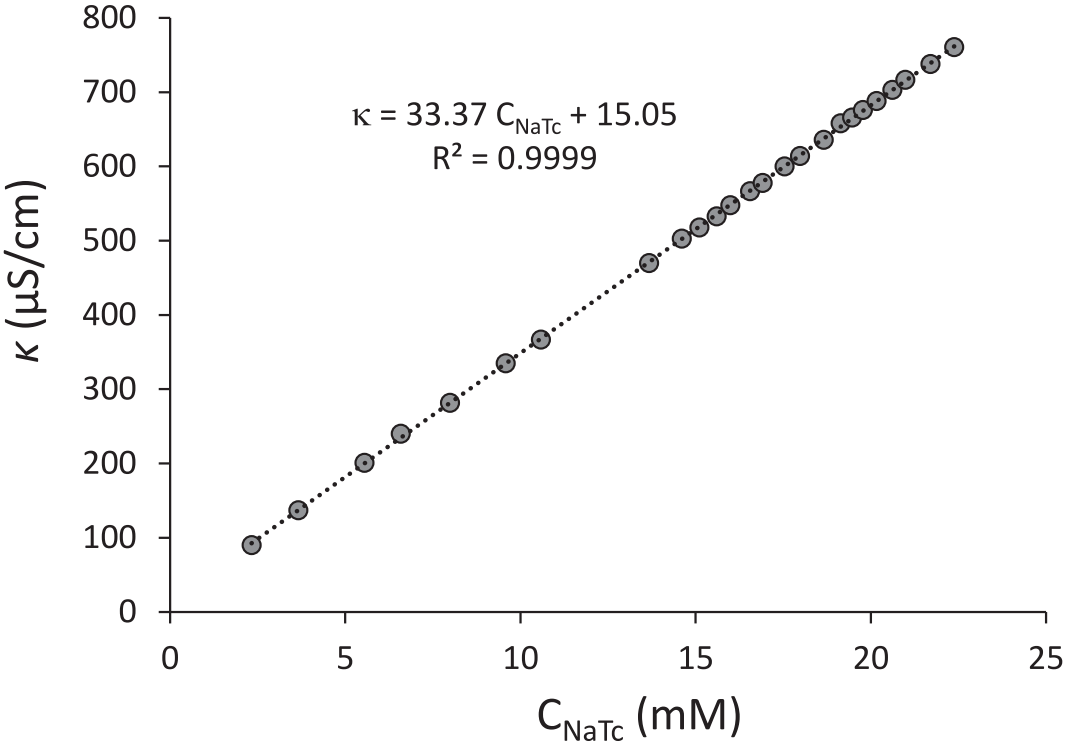

Fig. 2. κ *vs* C_{NaTc} plot in water at 25 °C.

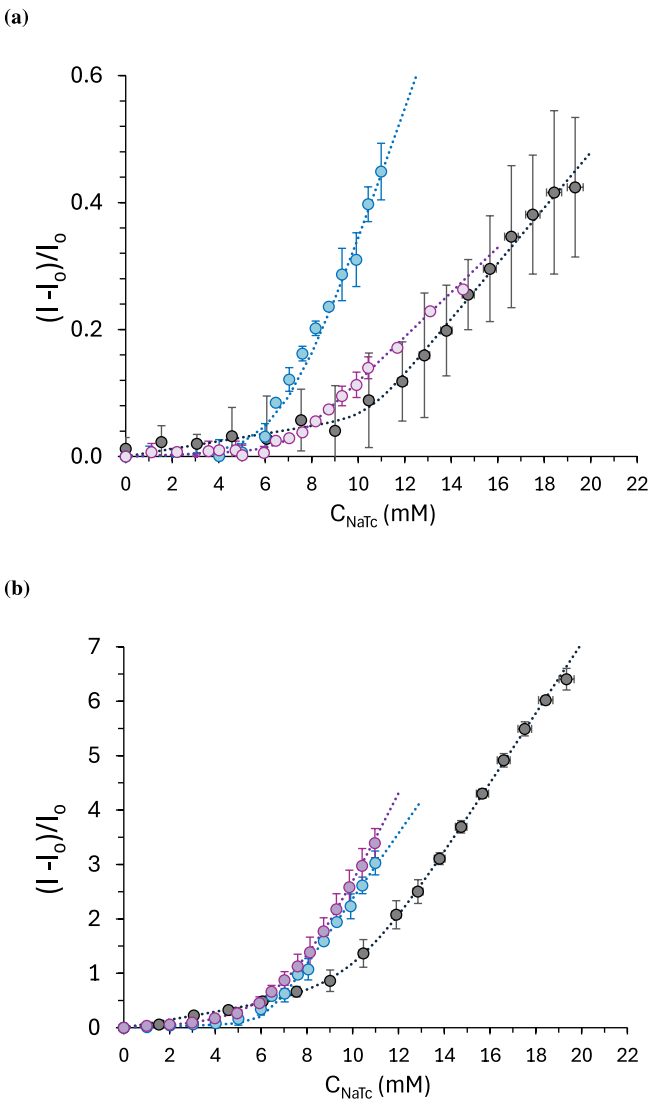

Fig. 3. I *vs* C_{NaTc} in water (black), maleic buffer pH 6.5 (I = 140 mM) (purple), maleic buffer pH 5.8 (I = 320 mM) (blue) using as fluorophore: propranolol (a) and tetracaine (b); Carpena's fitting models.

surfactant. Afterwards, when the surfactant micelles are putatively formed, the fluorescence intensity shows an increase. Curvature changes can be appreciated in all cases, although they are more pronounced when using tetracaine as probe. Therefore, the CMC (breaking point) can be obtained by fitting Eq. (1) to the experimental data (Table 2).

As shown in Table 2, the CMC in water at 25 °C is ~ 10.6 and comparable with the values reported in the literature at the same temperature (8–12 mM) (Table 1). The aggregation does not occur instantly but in a given concentration range, indeed the average transition range in water ($\Delta C_{D,NaTc}$ = 1.0 (0.3) mM) is wider than that of SDS ($\Delta C_{D,SDS}$ = 0.4 (0.1) mM) (Table A.3 and Fig. A.1.b – Supplementary material) and, hence, the aggregation of the monomers of NaTc is more gradual.

In the case of buffers that mimic the pH and ion strength of intestinal fluids in fasted (pH 6.5, *I* = 140 mM) and fed state (pH 5.8, *I* = 320 mM) (Fig. 3), the CMC is similar (~ 7 mM) but lower than the one determined in water. Here, the ion strength allows the micelles to aggregate sooner, as generally observed in different types of surfactants [31,32]. Although the two buffers used have different *I* value, CMC is similar because, as already observed in other studies considering different amounts of NaCl [28,31], when media with high amounts of salts are used the impact of the ion strength on the micellization process is softened (Table 1 and Fig. A.2 – Supplementary material).

The CMC was also determined in biorelevant media (FaSSIF-v2 and FeSSIF-v2) (Fig. 4). It can be clearly observed that in the presence of additional components the behavior of the fluorescence intensity changes. In these two cases, there is a fluorescence intensity enhancement when the first additions of simulated intestinal fluid (SIF) (NaTc + phospholipids/oils) are done. Hence, the probe starts to interact immediately with one or several components of system involving an impact on the environment and on the fluorescence intensity of the probe. When micelles are formed and the probe is fully incorporated into the mixed micelles structure, the environment of the probes changes again, and the fluorescence enhancement is not so pronounced.

Concerning the different probes, here, the curvature changes are more pronounced when using propranolol and provide more accurate results (Table 2). Indeed, the CMC values obtained using tetracaine in FaSSIF-v2 are not reproducible between replicates due to the difficulties in detecting the curvature change and only an approximate CMC value can be provided.

The CMC value using biorelevant media is lower than the value obtained when using solely the corresponding maleic buffers. Hence, the additional components (lecithin and, in the case of FeSSIF-v2 also lipids) with hydrophobic tails act synergistically [33] and help NaTc to form micelles at lower concentrations and to stabilize faster (ΔC_D ~ 0.5 mM in biorelevant media *vs* ΔC_D ~ 1 mM in water and in aqueous buffers).

Focusing on the methodology, it is important to note that the selection of an adequate fluorophore is key for having accurate results, and different probes have to be considered when facing studies on new solution media.

3.3. Calorimetry

Calorimetric experiments were first performed at 25 °C by adding the surfactant to a calorimetric cell containing water. Similar to conductometry and fluorescence assays, the surfactant concentration (250 mM) is higher than CMC and, therefore, NaTc is mainly in the form of micelles. Fig. 5a (blue curve) shows the variation of the enthalpy increment throughout injections in water at 25 °C. During the first ones, an initial endothermic process is observed. The principal contribution to the enthalpy (ΔH) change can be attributed to the breakdown of the micelles when they are diluted in the cell to a concentration under the CMC, that would result in the exposure of non-polar groups to the medium, and, in consequence, to the absorption of heat from the surrounding water. Also, the monomers dilution would have an influence on the endothermic event [31,34]. In the second part of the plot, a decreasing curve corresponding to another endothermic process is noticed. After the addition of higher amounts of NaTc, micelles would no longer break down and would coexist with monomers in the calorimetric cell. The transition between the two different behaviors is not so pronounced in the case of SDS (Table A.3 and Fig. A.1.c – Supplementary material). Again, this is an indication that micellization occurs more gradually for bile salts, and probably the monomers coexist with dimers, small aggregates, and micelles of different size [5,7]. After monitoring the enthalpy upon the addition of NaTc, CMC and other aggregation-related parameters were calculated using Eq. (2) (Table 2). At 25 °C, the calculated CMC is 13.3 (1.1) mM, and the heat steepest decrease occurs in a range of 3.5 (0.6) mM units around the CMC.

ITC instruments permit to control the temperature of titration experiments strictly and to evaluate thermodynamic parameters when working at different temperatures. Therefore, NaTc micellization was also studied at two biorelevant temperatures: 32 and 37 °C. As shown in Fig. 5a, the slope of the first zone corresponds to the heat involved in the demicellization and the dilution of the free monomers. These processes occur in less orderly manner when temperature increases. The second zone corresponds to the micellar region after the addition of higher amounts of concentrated surfactant. As shown in Table 2, at the three temperatures evaluated, there are no significant differences for CMC and ΔC_{NaTc}. Grijalva-Bustamante [24] did not observe significant variation

Table 2
Aggregation parameters of NaTc in water and aqueous media that mimic intestinal fluids using fluorescence and ITC.

Surfactant	Medium	Temperature	Technique	Probe	CMC (mM)	ΔC_D (mM)	ΔH_{mic} (kcal/mol)
NaTc	Water	25 °C	Fluorescence[a]	Propranolol	10.9 (0.8)	0.8 (0.2)	
				Tetracaine	10.2 (0.2)	1.2 (0.3)	
			ITC	None	13.3 (1.1)	3.5 (0.6)	−0.08 (0.02)
		32 °C	ITC	None	13.3 (1.8)	4.4 (0.7)	−0.32 (0.04)
		37 °C	ITC	None	13.2 (1.7)	4.1 (0.2)	−0.49 (0.03)
NaTc	Maleic buffer (I = 140 mM, pH 6.5)	25 °C	Fluorescence[a]	Propranolol	7.1 (0.6)	0.8 (0.2)	
				Tetracaine	7.1 (0.4)	1.1 (0.3)	
			ITC	None	6.8 (0.2)	2.5 (0.2)	−0.08 (0.01)
		32 °C	ITC	None	6.6 (0.6)	2.2 (0.2)	−0.36 (0.05)
		37 °C	ITC	None	6.1 (0.7)	2.4 (0.2)	−0.70 (0.09)
NaTc	Maleic buffer (I = 320 mM, pH 5.8)	25 °C	Fluorescence	Propranolol	6.7 (0.4)	0.8 (0.2)	
				Tetracaine	6.8 (0.3)	0.9 (0.2)	
			ITC	None	7.2 (0.4)	2.1 (0.2)	−0.05 (0.02)
		32 °C	ITC	None	5.8 (0.2)	2.1 (0.2)	−0.42 (0.01)
		37 °C	ITC	None	5.7 (0.5)	2.0 (0.1)	−0.54 (0.07)
FaSSIF-v2	Maleic buffer (I = 140 mM, pH 6.5)	25 °C	Fluorescence	Propranolol	3.8 (0.4)	0.9 (0.4)	
				Tetracaine	~ 3		
			ITC	None	4.2 (0.3)	1.4 (0.1)	−0.31 (0.07)
		32 °C	ITC	None	4.5 (0.4)	1.4 (0.1)	−0.87 (0.13)
		37 °C	ITC	None	4.2 (0.3)	1.4 (0.1)	−1.36 (0.07)
FeSSIF-v2	Maleic buffer (I = 320 mM, pH 5.8)	25 °C	Fluorescence	Propranolol	2.8 (0.4)	0.4 (0.2)	
				Tetracaine	2.9 (0.3)	0.5 (0.3)	
			ITC	None	5.3 (0.1)	0.3 (0.1)	−0.39 (0.01)
		32 °C	ITC	None	5.4 (0.2)	0.3 (0.1)	−0.69 (0.01)
		37 °C	ITC	None	5.8 (0.1)	0.5 (0.1)	−1.16 (0.01)

[a] Published in[30].

in the range 10–40 °C by osmometry, either. At 37 °C, the CMC value agrees with the one reported by Pigliacelli *et al.* [35] using NMR (Table 1).

Concerning the enthalpy involved in the micellization process (ΔH_{mic}), the endothermic event is higher when increasing the temperature. In fact, the following linear relationship has been observed:

$$\Delta H_{mic} = -0.034(0.001)\ T + 10.1(0.1);\ R^2 = 0.999 \quad (3)$$

where the slope (−0.0340 kcal mol^{-1} K^{-1}) characterizes the heat capacity change upon micellization ($\Delta C_{p,mic}$).

When ITC experiments are performed using aqueous buffers (Fig. 5b), the CMC values are ~ 7 mM at 25 °C. When temperature is increased, a slight trend towards lower micellization concentrations is observed for maleic buffer pH 6.5 (I = 140 mM)), and more pronounced for maleic buffer pH 5.8 (I = 320 mM). Here, temperature could favor the reorganization of molecules in a faster way. Further, and as already observed in the experiments performed in water, the process is endothermic, and the heat required increases with temperature (Eq. 4 refers to maleic buffer pH 6.5 (I = 140 mM) and Eq. 5 to maleic buffer pH 5.8 (I = 320 mM).

$$\Delta H_{mic} = -0.050(0.008)\ T + 1.2(0.2);\ R^2 = 0.977 \quad (4)$$

$$\Delta H_{mic} = -0.054(0.004)\ T + 1.3(0.1);\ R^2 = 0.964 \quad (5)$$

Finally, in the experiments done using biorelevant media (Fig. 5c), the micelles are formed at lower concentrations of surfactant and without remarkable differences at the range of temperatures considered, but the presence of lecithin and other components makes the micellization occur sooner (CMC ~ 4.3 mM for FaSSIF-v2 and CMC ~ 5.5 mM for FeSSIF-v2). In the case of FaSSIF-v2, the thermodynamic behavior is erratic below the CMC. Here, the reorganization process between NaTc and lecithin would not be homogenous until micelles are formed. In the case of FeSSIF-v2, the presence of oils would facilitate a more uniform restructuration due to synergistic effects [33]. Concerning the range of concentrations where the micellization occurs, this process (ΔC_D = 2.1 (0.2) mM) is similar to the one in aqueous buffers (ΔC_D = 2.4 (0.2) mM) but less stepwise than in the case of water (ΔC_D = 4.0 (0.5) mM).

Regarding the thermodynamic process, it is endothermic (Eq. 6 for FaSSIF-v2 and Eq. 7 for FeSSIF-v2), and the heat capacity change upon micellization ($\Delta C_{p,mic}$) becomes more negative as CMC value decreases.

$$\Delta H_{mic} = -0.087(0.005)\ T + 1.9(0.2);\ R^2 = 0.997 \quad (6)$$

$$\Delta H_{mic} = -0.063(0.01)\ T + 1.2(0.4);\ R^2 = 0.951 \quad (7)$$

3.4. Comparison of techniques

When comparing the results obtained by fluorescence and ITC in water (Table 2), it can be observed that the NaTc concentrations where the physical property undergoes a variation are lower in the case of fluorescence for the experiments performed. We also observed the same phenomenon but in a lesser extent when evaluating the micellization of SDS (6.9 (0.6) mM by fluorescence and 8.2 (0.1) mM by ITC) (–Table A.3 Supplementary material), a conventional surfactant that aggregates faster. As the experiments on NaTc had also been carried out previously in the absence of probes [30], the possible influence on the micellization process of an external artifact was discarded. Hence, the differences may be related to the physical property monitored, and may not indicate incorrect but complementary results. Possibly, the change of the electronic properties of the system that occurs during the micellization process and that affects the fluorophores behavior takes place at lower surfactant concentrations than the thermodynamic changes.

As regards the range of concentrations where the aggregation process takes place, SDS shows the same range independently of the technique (ΔC_D = 0.4 (0.1) mM at 25 °C, Table A.3 – Supplementary material). However, for NaTc the values are, in all conditions considered, higher when using ITC (Table 2). Therefore, calculated ΔC_D values obtained by both techniques are comparable for surfactants whose monomers aggregate simultaneously but they are not in the case of those that aggregate gradually. In this last case, the physical change observed by fluorescence occurs in a narrower period than that observed monitoring the enthalpy increment. Calorimetry would monitor the whole gradual NaTc micellization process. On its behalf, fluorescence would detect the initial micellization steps as fluorophores rapidly achieve a constant fluorescence intensity when this aggregation process starts.

Further, when we compared our results with those reported in the literature, we observed that the values obtained for NaTc using

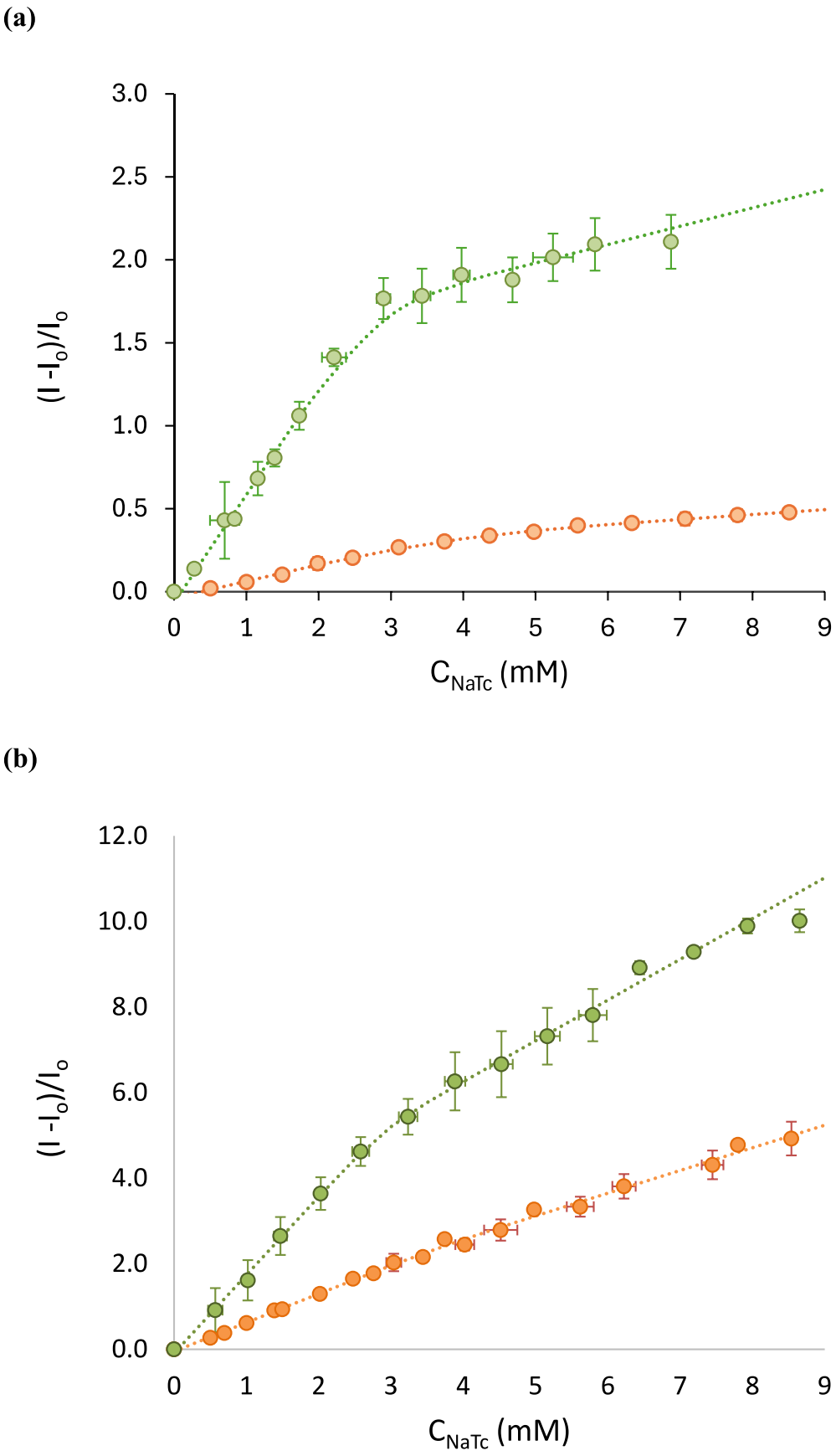

Fig. 4. I *vs* C_{NaTc} in FaSSIF-v2 (orange) and FeSSIF-v2 (green) using as fluorophore: propranolol (a) and tetracaine (b); Carpena's fitting models.

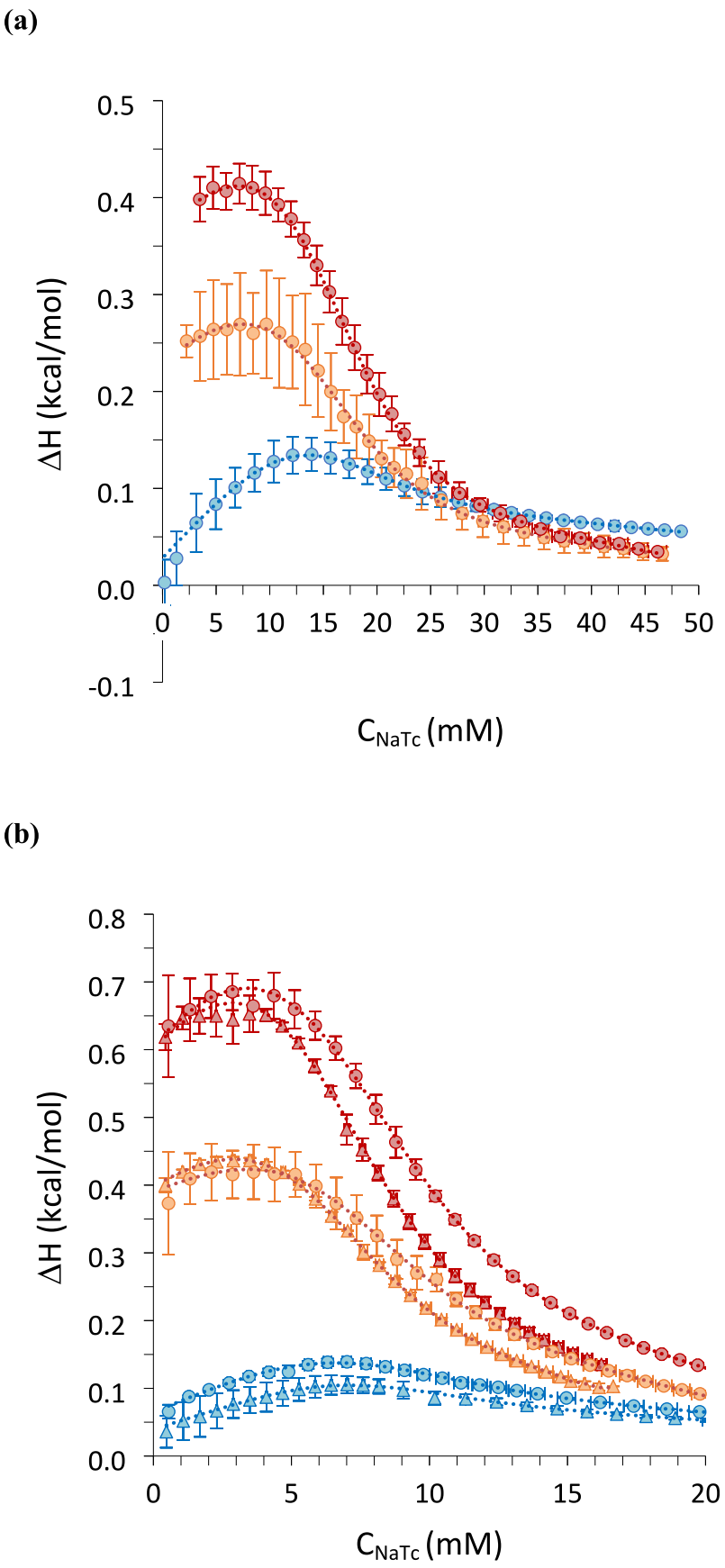

Fig. 5. ΔH *vs* C_{NaTc} and model fitting using D/STAIN program at 37 °C (red), 32 °C (orange) and 25 °C (blue) in: (a) water, (b) aqueous buffers [maleic buffer pH 6.5 (I = 140 mM) (circles), maleic buffer pH 5.8 (I = 320 mM) (triangles)], and (c) biorelevant media [FaSSIF-v2 (circles), and FeSSIF-v2 (triangles)]. (For interpretation of the references to colour in this figure legend, the reader is referred to the web version of this article.)

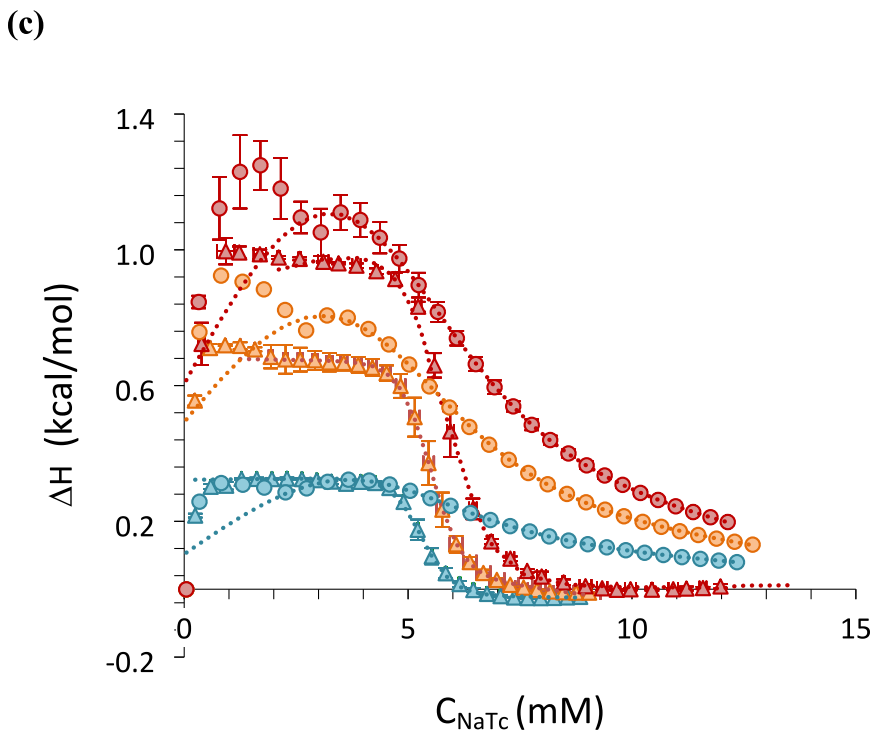

Fig. 5. (*continued*).

osmometry in water (6.1 – 6.8 mM at temperatures ranging from 10 to 40 °C) [34] or in buffer [34] were even lower than those observed by fluorescence or ITC. Hence, osmometry would be a sensitive technique for the evaluation of the beginning of the micellization process.

In the case of the micellization in maleic buffers, we did not observe significant differences between fluorescence and ITC (Table 2); probably ion strength homogenizes both aggregation and changes occurring in the fluorophore environment. This phenomenon was also observed in FaSSIF-v2 but not in FeSSIF-v2. In order to deep in the understanding of the role of the probes in the obtained results, we decided to evaluate CMC in these two media using fluorescence without markers and we screened directly NaTc signal at 25 °C. We prepared more than 10 replicates and we observed that, even if the experiments were not reproducible after smooth work, the CMC was in the range 2–6 mM for FaSSIF-v2, range that includes the CMC values obtained by both fluorescence and calorimetry. In the case of FeSSIF-v2, the CMC was 4–7 mM, range that includes the CMC values obtained only by calorimetry. Therefore, in this specific case, the probe (propranolol or tetracaine) undergoes fluorescence intensity changes before NaTc does. As long as FeSSIF-v2 contains several lipids and, hence, forms more complex mixed micelles than FaSSIF-v2, where only lecithin is incorporated into NaTc micellar structure, the fluorophores' environment could be modified substantially even before detecting the heat exchange modification due to micellization. As far as we are concerned, literature only refers to one study of micellization of FeSSIF. Gómez *et al.* [36],evaluated CMC of a fed-state simulated fluid containing NaTc and lecithin in acetic acid buffer (pH 5.0, $I = 320$ mM). Ibuprofen solubilization thermodynamics led to a CMC value of 3.4 mM. As this medium does not contain lipids, CMC is more similar to that observed in the present study for FaSSIF-v2 than for FeSSIF-v2, indicating that these compounds play a role in the structure and formation of NaTc simple and mixed micelles.

4. Conclusions

Sodium taurocholate is a surfactant with special relevance in gastrointestinal fluids due to its ability to incorporate in its micelles low-soluble drugs and to improve their bioavailability. However, the structure of its micelles and the way it aggregates is still under discussion. In the present work we have compared the usefulness for the evaluation of the aggregating behavior of different analytical techniques. The physical properties monitored undergo a variation of CMC values from 10 to 14 mM in water, and are not significantly affected by temperature or, in the case of fluorescence, by the fluorophore used. The CMC in maleic buffers at biorelevant conditions of pH and ionic strength is ~ 7 mM, in FaSSIF-v2 is ~ 4 mM, and in FeSSIF-v2 is ~ 5 mM. Thus, when considering intestinal conditions, it can be observed that micellization is favored not only by the biorelevant ion strength but also by the presence of other components of the fluids (phospholipids and lipids).

Conductometry has shown not to be sensitive enough for biliary salts CMC characterization. Fluorescence and ITC provide complementary information of the aggregation of NaTc monomers until the most stable micelles are formed. Fluorescence would be indicative of the beginning of the micellization while ITC would monitor the whole process. Special attention has to be given to fluorophores selected for fluorescence enhancement studies as they may not have the same sensitivity and behavior in different media.

CRediT authorship contribution statement

Susana Amézqueta: Writing – original draft, Visualization, Project administration, Methodology, Investigation, Conceptualization. **Unai Casanova:** Investigation. **Elisabet Fuguet:** Writing – review & editing, Visualization, Funding acquisition, Conceptualization. **Clara Ràfols:** Writing – original draft, Visualization, Project administration, Methodology, Formal analysis, Conceptualization.

Declaration of competing interest

The authors declare that they have no known competing financial interests or personal relationships that could have appeared to influence the work reported in this paper.

Acknowledgements

This publication is part of the R&D&I project PID2023-150245NB-I00, funded by MICIU/AEI/10.13039/501100011033/ and ERDF/EU. Support from the Catalan Government (2021SGR00248) is also acknowledged.

Appendix A. Supplementary data

Supplementary data to this article can be found online at https://doi.org/10.1016/j.microc.2025.113934.

Data availability

Data will be made available on request.

References

[1] A. Macierzanka, A. Torcello-Gómez, C. Jungnickel, J. Maldonado-Valderrama, Bile salts in digestion and transport of lipids, Adv Colloid Interface Sci 274 (2019) 102045, https://doi.org/10.1016/j.cis.2019.102045.
[2] A.L. Bose, D. Bhattacharjee, D. Goswami, Mixed micelles and bicontinuous microemulsions: Promising media for enzymatic reactions, Colloids Surf B Biointerfaces 209 (2022) 112193, https://doi.org/10.1016/j.colsurfb.2021.112193.
[3] R.B. Yu, J.P. Quirino, Bile salts in chiral micellar electrokinetic chromatography: 2000–2020, Molecules 26 (2021) 5531, https://doi.org/10.3390/molecules26185531.
[4] K. Baker, R. Sikkema, W. Liang, I. Zhitomirsky, Multifunctional properties of commercial bile salts for advanced materials engineering, Adv Eng Mater 23 (2021) 2001261, https://doi.org/10.1002/adem.202001261.
[5] N.A. Malik, Solubilization and Interaction Studies of Bile Salts with Surfactants and Drugs: a Review, Appl Biochem Biotechnol 179 (2016) 179–201, https://doi.org/10.1007/s12010-016-1987-x.
[6] M.C. Di Gregorio, L. Travaglini, A. Del Giudice, J. Cautela, N.V. Pavel, L. Galantini, Bile Salts: Natural Surfactants and Precursors of a Broad Family of Complex Amphiphiles, Langmuir 35 (2019) 6803–6821, https://doi.org/10.1021/acs.langmuir.8b02657.
[7] P.Y. Parekh, V.I. Patel, M.R. Khimani, P. Bahadur, Self-assembly of bile salts and their mixed aggregates as building blocks for smart aggregates, Adv Colloid Interface Sci (2023) 102846, https://doi.org/10.1016/j.cis.2023.102846.
[8] D.B. Warren, D.K. Chalmers, K. Hutchison, W. Dang, C.W. Pouton, Molecular dynamics simulations of spontaneous bile salt aggregation, Colloids Surf A Physicochem Eng Asp 280 (2006) 182–193, https://doi.org/10.1016/j.colsurfa.2006.02.009.
[9] P. Carpena, J. Aguiar, P. Bernaola-Galván, C. Carnero Ruiz, Problems associated with the treatment of conductivity-concentration data in surfactant solutions: Simulations and experiments, Langmuir 18 (2002) 6054–6058, https://doi.org/10.1021/la025770y.
[10] J.M. Goronja, A.M.J. Ležaić, B.M. Dimitrijević, A.M. Malenović, D.R. Stanisavljev, N.D. Pejić, Determination of critical micelle concentration of cetyltrimethylammonium bromide: Different procedures for analysis of experimental data, Hem Ind 70 (2016) 485–492, https://doi.org/10.2298/HEMIND150622055G.
[11] S.C. Tso, F. Mahler, J. Höring, S. Keller, C.A. Brautigam, Fast and robust quantification of detergent micellization thermodynamics from isothermal titration calorimetry, Anal Chem 92 (2020) 1154–1161, https://doi.org/10.1021/acs.analchem.9b04281.
[12] A. Maestre, P. Guardado, M.L. Moyá, Thermodynamic study of bile salts micellization, J Chem Eng Data 59 (2014) 433–438, https://doi.org/10.1021/je400903n.
[13] J. Rosenberger, J. Butler, J. Dressman, A refined Developability Classification System, J Pharm Sci 107 (2018) 2020–2032, https://doi.org/10.1016/j.xphs.2018.03.030.
[14] P. Augustijns, B. Wuyts, B. Hens, P. Annaert, J. Butler, J. Brouwers, A review of drug solubility in human intestinal fluids: implications for the prediction of oral absorption, Eur. J. Pharm. Sci. 57 (2014) 322–332, https://doi.org/10.1016/j.ejps.2013.08.027.
[15] K. Nakamura, A. Kambayashi, S. Onoue, Importance of Considering Fed-State Gastrointestinal Physiology in Predicting the Reabsorption of Enterohepatic Circulation of Drugs, Pharm Res 41 (2024) 673–685, https://doi.org/10.1007/s11095-024-03669-3.
[16] F. Mustan, A. Ivanova, S. Tcholakova, Taurodeoxycholate Aggregation Explored by Molecular Dynamics: Primary-To-Secondary Micelle Transition and Formation of Mixed Micelles with Fatty Acids, Molecules 29 (2024), https://doi.org/10.3390/molecules29245897.
[17] Biorelevant, Biorelevant Media, (2025). https://biorelevant.com/ (accessed March 30, 2025).
[18] J.L. Beltrán, J.J. Pignatello, M. Teixidó, ISOT_Calc: A versatile tool for parameter estimation in sorption isotherms, Comput Geosci 94 (2016) 11–17, https://doi.org/10.1016/j.cageo.2016.04.008.
[19] M. Textor, S. Keller, Automated analysis of calorimetric demicellization titrations, Anal Biochem 485 (2015) 119–121, https://doi.org/10.1016/j.ab.2015.06.009.
[20] J. Broecker, S. Keller, Impact of urea on detergent micelle properties, Langmuir 29 (2013) 8502–8510, https://doi.org/10.1021/la4013747.
[21] S. Keller, C. Vargas, H. Zhao, G. Piszczek, C.A. Brautigam, P. Schuck, High-precision isothermal titration calorimetry with automated peak-shape analysis, Anal Chem 84 (2012) 5066–5073, https://doi.org/10.1021/ac3007522.
[22] Https://www.utsouthwestern.edu/research/core-Facilities/mbr/software/ (2025).
[23] E. Fuguet, C. Ràfols, M. Rosés, E. Bosch, Critical micelle concentration of surfactants in aqueous buffered and unbuffered systems, Anal Chim Acta 548 (2005) 95–100, https://doi.org/10.1016/j.aca.2005.05.069.
[24] B. Mukherjee, A.A. Dar, P.A. Bhat, S.P. Moulik, A.R. Das, Micellization and adsorption behaviour of bile salt systems, RSC Adv 6 (2016) 1769–1781, https://doi.org/10.1039/c5ra20909a.
[25] B. Natalini, R. Sardella, A. Gioiello, F. Ianni, A. Di Michele, M. Marinozzi, Determination of bile salt critical micellization concentration on the road to drug discovery, J Pharm Biomed Anal 87 (2014) 62–81, https://doi.org/10.1016/j.jpba.2013.06.029.
[26] G. Li, L.B. McGown, Model for Bile Salt Micellization and Solubilization from Studies of a "Polydisperse" Array of Fluorescent Probes and Molecular Modeling, J Phys Chem 98 (1994) 13711–13719, https://doi.org/10.1021/j100102a043.
[27] S.M. Meyerhoffer, L.B. McGown, Critical micelle concentration behavior of sodium taurocholate in water, Langmuir 6 (1990) 187–191, https://doi.org/10.1021/la00091a030.
[28] K. Matsuoka, M. Maeda, Y. Moroi, Micelle formation of sodium glyco- and taurocholates and sodium glyco- and taurodeoxycholates and solubilization of cholesterol into their micelles, Colloids Surf B Biointerfaces 32 (2003) 87–95, https://doi.org/10.1016/S0927-7765(03)00148-6.
[29] J. Aguiar, P. Carpena, J.A. Molina-Bolívar, C. Carnero Ruiz, On the determination of the critical micelle concentration by the pyrene 1:3 ratio method, J Colloid Interface Sci 258 (2003) 116–122, https://doi.org/10.1016/S0021-9797(02)00082-6.
[30] S. Amézqueta, E. Fuguet, R. Cabañas, C. Ràfols, Characterization of biosurfactants' micelles formation using fluorescence measurements: sodium taurocholate as case of study, ADMET DMPK 12 (2024) 769–780, https://doi.org/10.5599/admet.2322.
[31] M. Thongngam, D.J. McClements, Isothermal titration calorimetry study of the interactions between chitosan and a bile salt (sodium taurocholate), Food Hydrocoll 19 (2005) 813–819, https://doi.org/10.1016/j.foodhyd.2004.11.001.
[32] P. Palladino, R. Ragone, Ionic strength effects on the critical micellar concentration of ionic and nonionic surfactants: The binding model, Langmuir 27 (2011) 14065–14070, https://doi.org/10.1021/la202897q.
[33] S. Kumar Shah, G. Chakraborty, A. Bhattarai, R. De, Synergistic and antagonistic effects in micellization of mixed surfactants, J Mol Liq 368 (2022), https://doi.org/10.1016/j.molliq.2022.120678.
[34] G.A. Grijalva-Bustamante, R.V. Quevedo-Robles, T. del Castillo-Castro, M. M. Castillo-Ortega, J.C. Encinas, D.E. Rodríguez-Félix, T.E. Lara-Ceniceros, D. Fernández-Quiroz, J. Lizardi-Mendoza, L. Armenta-Villegas, A novel bile salt-assisted synthesis of colloidal polypyrrole nanoparticles, Colloids Surf A Physicochem Eng Asp 600 (2020) 124961, https://doi.org/10.1016/j.colsurfa.2020.124961.
[35] C. Pigliacelli, P. Belton, P. Wilde, S. Qi, Probing the molecular interactions between pharmaceutical polymeric carriers and bile salts in simulated gastrointestinal fluids using NMR spectroscopy, J Colloid Interface Sci 551 (2019) 147–154, https://doi.org/10.1016/j.jcis.2019.05.002.
[36] S.M. Gómez, D.M. Cristancho, F. Martínez, Solubilization thermodynamics of ibuprofen in modified and classical FeSSIF biorelevant media, J Mol Liq 179 (2013) 110–117, https://doi.org/10.1016/j.molliq.2012.12.010.
[37] N. Funasaki, M. Fukuba, T. Kitagawa, M. Nomura, S. Ishikawa, S. Hirota, S. Neya, Two-dimensional NMR study on the structures of micelles of sodium taurocholate, J. Phys. Chem. B 108 (2004) 438–443, https://doi.org/10.1021/jp030899h.
[38] G. Ravidiandjran, Acoustical studies on the effect of urea on the micelles of aqueous surfactants, Indian J. Phys 76 (2002) 277–282. https://core.ac.uk/download/pdf/159339872.pdf.
[39] K. Ryu, J.M. Lowery, D.F. Evans, E.L. Cussler, Studies of model bile solutions using surfactant ion electrodes, J. Phys. Chem. 87 (1983) 5015–5019, https://doi.org/10.1021/j150642a048.
[40] G.A. Grijalva-Bustamante, R.V. Quevedo-Robles, T. del Castillo-Castro, M. M. Castillo-Ortega, J.C. Encinas, D.E. Rodríguez-Félix, T.E. Lara-Ceniceros, D. Fernández-Quiroz, J. Lizardi-Mendoza, L. Armenta-Villegas, A novel bile salt-assisted synthesis of colloidal polypyrrole nanoparticles, Colloids Surf A Physicochem Eng Asp 600 (2020), https://doi.org/10.1016/j.colsurfa.2020.124961.
[41] K. Andrieux, L. Forte, S. Lesieur, M. Paternostre, M. Ollivon, C. Grabielle-Madelmont, Insertion and partition of sodium taurocholate into egg phosphatidylcholine vesicles, Pharm Res 21 (2004) 1507, https://doi.org/10.1023/B:PHAM.0000036927.37888.93.
[42] C. de Oliveira, B. Khatua, B. El-Kurdi, K. Patel, V. Mishra, S. Navina, B.J. Grim, S. Gupta, M. Belohlavek, B. Cherry, J. Yarger, M.D. Green, V.P. Singh, Thermodynamic interference with bile acid demicelleization reduces systemic entry and injury during cholestasis, Sci Rep 10 (2020) 1–15, https://doi.org/10.1038/s41598-020-65451-w.
[43] Y. Chang, J.R. Cardinal, Light-scattering studies on bile acid salts I: Pattern of self-association of sodium cholate, sodium glycocholate, and sodium taurocholate in aqueous electrolyte solutions, J Pharm Sci 67 (1978) 174–181, https://doi.org/10.1002/jps.2600670214.